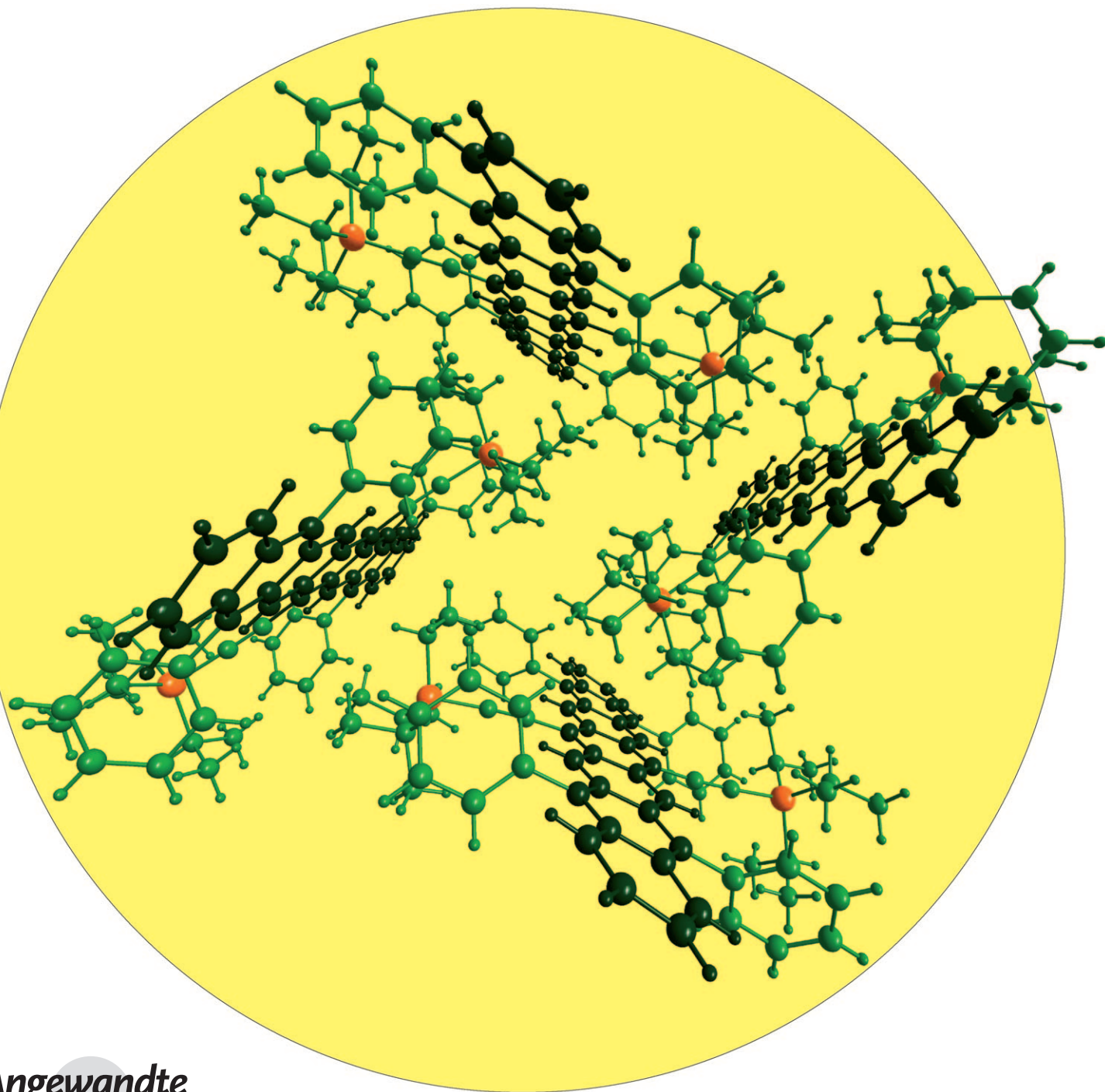


The Most Stable and Fully Characterized Functionalized Heptacene**

*Doris Chun, Yang Cheng, and Fred Wudl**



Angewandte
Chemie

8508

WILEY
InterScience®
DISCOVER SOMETHING GREAT

© 2008 Wiley-VCH Verlag GmbH & Co. KGaA, Weinheim

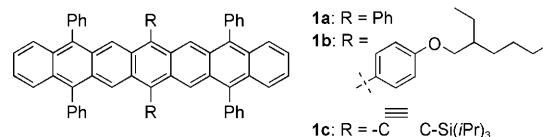
Angew. Chem. 2008, 120, 8508–8513

Linear polyacenes **2** are one of the most fascinating classes of organic molecules.^[1,2] Benzene (**2**, $n=1$), the smallest member of the family, is the most stable known aromatic hydrocarbon. Since the discovery of benzene in the fractional distillation of coal extracts by Faraday in 1825,^[3] naphthalene (**2**, $n=2$) and anthracene (**2**, $n=3$), were also isolated from coal-tar and petroleum distillates.^[1] The higher homologues (**2**, $n>3$) however, are not found in nature and can be obtained only through multi-step syntheses. The electronic coupling of their extensively delocalized π orbitals in the solid state means that these linearly fused polycyclic aromatic hydrocarbons (PAHs) are intrinsic semiconductors.

Theoretical calculations predict a narrowing of band gap energies in the acene family with each successive benzene ring addition up to hexacene, beyond which the HOMO–LUMO (HOMO = highest occupied molecular orbital, LUMO = lowest unoccupied molecular orbital) gap remains constant because of the emergence of a singlet biradical character in the ground state.^[4,5] Hence, the electronic properties of the longer acenes have long been a subject of debate.^[6] While the physical properties of the smaller linear PAHs (**2** with $n \leq 5$) are well explored, our knowledge of longer acenes is limited for two major reasons: 1) the synthetic challenge in their production and their insolubility and 2) their extreme instability with increased length, which makes them characterizable only by electronic spectroscopy in a matrix at low temperatures. Neckers and co-workers have reported stability studies of hexacene and heptacene generated photochemically in PMMA matrix.^[7,8] However, these molecules could not be isolated and they are stable for only a few hours when protected by the polymer matrix.^[7,8] An effective approach to stabilize and solubilize long PAHs was demonstrated by Anthony and co-workers who strategically functionalized the acene backbone with alkylsilyl ethynyl groups.^[9]

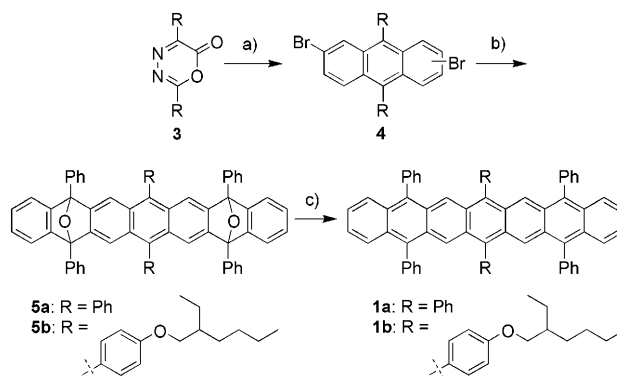
The most common synthetic route to functionalized polyacenes is through the nucleophilic addition of organo-metallic reagents to an acene quinone, followed by reduction

to afford the desired product.^[10–15] We explored other methodologies to provide a new route to functionalized higher acenes. To the best of our knowledge, the work reported herein is the first report of a double Diels–Alder cycloaddition between a lateral “bisanthracene” and dienes, followed by reduction to give heptacene derivatives **1a–c** (Scheme 1).



Scheme 1. The molecular structure of heptacene derivatives **1a–c**.

The 2,5-diaryl-6-oxo-1,3,4-oxadiazine-6-one **3**^[16] is an electron-deficient diene that undergoes an inverse-electron-demand Diels–Alder reaction twice with benzyne to give the resulting anthracene derivative **4**.^[17] Trapping of the “bisanthracene” (generated through sequential dehydrohalogenation of dibromide **4**) with diphenylisobenzofuran afforded bis-*endo*-oxide **5**. Metal reduction of **5** provided the expected functionalized heptacenes **1a,b** (Scheme 2).



Scheme 2. a) 1. 5-bromoanthranilic acid, isoamyl nitrite, THF, 0°C. 2. DCE, reflux, 30%; b) Diphenylisobenzofuran, LTMP, THF, 0°C → RT, 32%; c) Fe metal, AcOH, *o*-DCB, 100°C. DCE = dichloroethane, LTMP = lithium tetramethylpiperide

Heptacene **1a** was insoluble even in aromatic solvents. It readily precipitated as a deep-green solid upon cooling the reaction mixture in *o*-dichlorobenzene (*o*-DCB; Figure 1). Attempts to dissolve **1a** in *o*-DCB by sonication and heating facilitated its oxidation to form an *endo*-peroxide. The UV/Vis spectrum of **1a** in *o*-DCB is very broad because of aggregation; nonetheless, the expected vibronic pattern at long wavelengths is present. Heptacene **1b** was synthesized in the same manner as **1a**, except the aryl hydrazide and aryl glyoxylic acid needed to be first synthesized. Although the alkoxy side chains significantly improved its solubility, **1b** was too reactive to obtain an electronic spectrum of the pure compound. Nonetheless, as shown in Figure 2, the vibronic pattern of **1a** and **1b** in the near-IR region is undoubtedly due to the presence of heptacene. The strong absorption with

[*] D. Chun
Department of Chemistry and Biochemistry, University of California
Los Angeles, CA 90095-1569 (USA)

D. Chun, Dr. Y. Cheng,^[†] Prof. Dr. F. Wudl
Department of Chemistry and Biochemistry 9510, University of
California
Santa Barbara, CA 93106-9510 (USA)
Fax: (+1) 805-893-4120
E-mail: wudl@chem.ucsb.edu
Homepage: www.chem.ucsb.edu/

[†] Current Address: Core Research & Development, The Dow
Chemical Company
Midland, MI 48674 (USA)

[**] We are indebted to Dr. Guan Wu for his assistance with the single-crystal structure elucidation. We thank Prof. John Anthony for providing valuable insight and data that helped facilitate our characterization. We also thank Prof. Galen Stucky for helpful suggestions which led to the successful collection of the X-ray data and Brittnee Veldman for technical assistance with the UV/Vis–NIR data. This work was funded by the NSF through grant DMR 9796302.

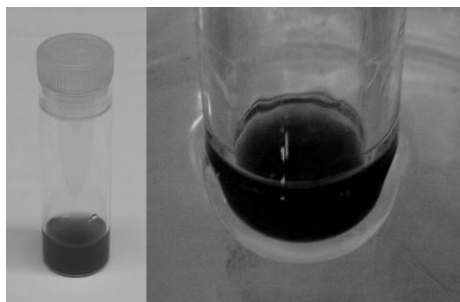


Figure 1. A suspension of 5,7,9,14,16,18-hexaphenyl heptacene **1a** in *o*-DCB (left) and a reaction mixture containing 5,9,14,18-tetraphenyl-7,16-bis[4-(2-ethylhexyloxy)phenyl]heptacene **1b** in toluene (right).

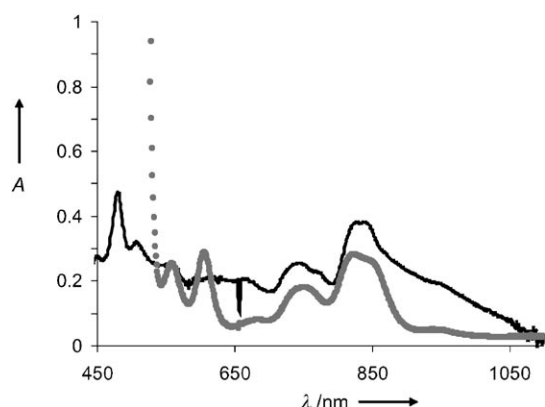
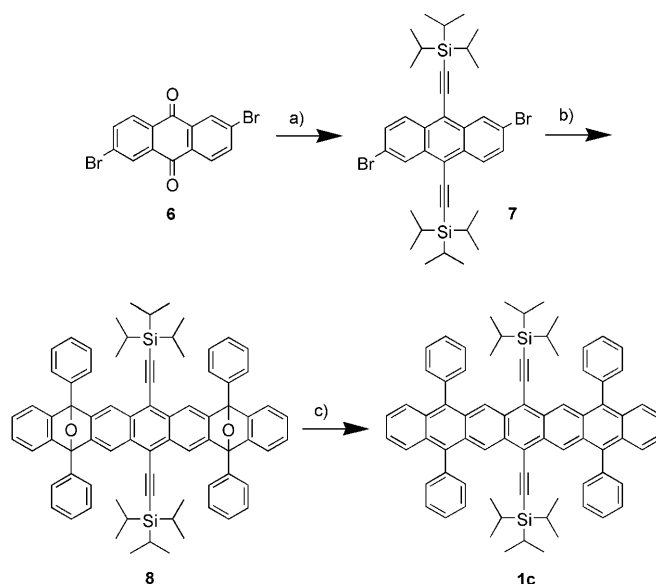


Figure 2. UV/Vis absorption spectra of **1a** (solid line) and **1b** (dotted line).

onset at 540 nm arises from the immediate oxidation of **1b** upon exposure to air and light, despite sample preparation under strictly anaerobic conditions. After 15 min, the color of the reaction mixture of **1b** changed from dark brown to bright orange and the UV/Vis spectrum showed a clear vibronic pattern, which indicated a tetracene-containing compound (Figure 3).

Among the three heptacene derivatives only **1c** was sufficiently stable to be isolated and characterized. It was synthesized from 2,6-dibromo-anthraquinone **6**^[18] in four

steps (Scheme 3). Unlike the metal reduction of **5**, bis-*endo*-oxide **8** did not undergo reduction under the same reaction conditions; a stronger reducing metal, zinc in this case, had to be used.



Scheme 3. a) 1. $i\text{Pr}_3\text{SiCCH}$, $n\text{BuLi}$, THF, 0°C –RT, 2. SnCl_2 , 50% AcOH, 86% overall; 3. LTMP, diphenylisobenzofuran, THF, -10°C →RT, 32%; c) Zn dust, AcOH, toluene, 100°C , 4 days, 73%.

Upon slow cooling in an oil bath, the reaction mixture of **1c** produced high-quality crystals for X-ray structural analysis (Figure 4). These opaque prismatic crystals are stable when coated with mineral oil even under constant exposure to the laboratory atmosphere and light for over 21 days. Interestingly, **1c** exhibits edge-to-face herringbone packing in the solid state (Figure 5), however there are no π – π interactions between the acene backbones. A stability study in toluene was accomplished by monitoring the disappearance of vibronic absorptions in the near-IR region (Figure 6). Heptacene **1c** is significantly more stable than any other heptacene derivatives synthesized to date: Its presence was still detectable by UV/Vis/NIR spectroscopy in degassed toluene after 41 h of exposure to air. When **1c** is dissolved in a degassed solvent

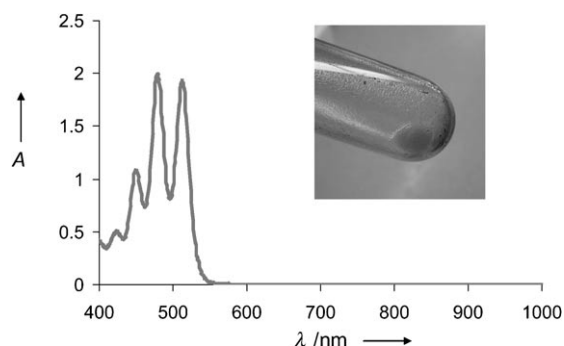


Figure 3. UV/Vis spectrum of **1b** 15 min after exposure to light and air. The exposed sample is orange, which indicates the presence of a tetracene species

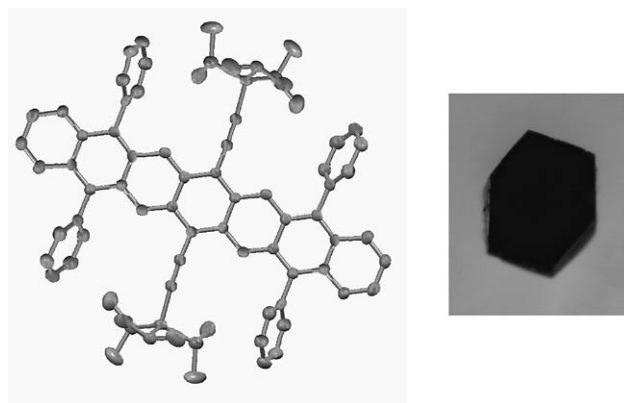


Figure 4. X-ray crystal structure and the single crystal of heptacene **1c**.

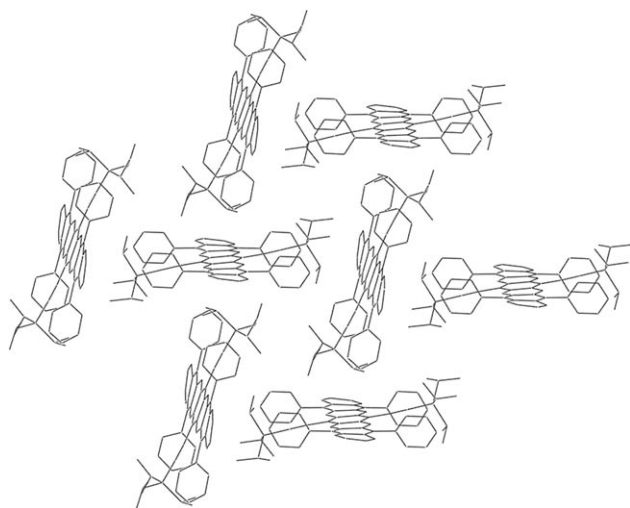


Figure 5. The herringbone packing motif of **1c**.

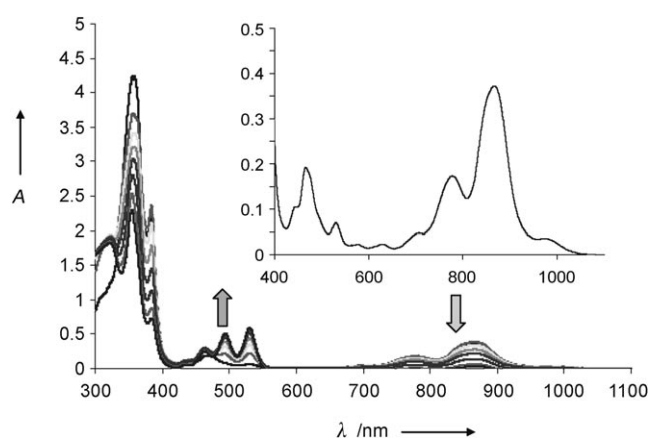
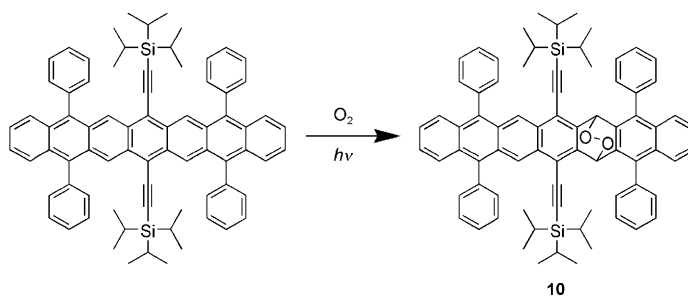


Figure 6. Degradation study of **1c** in toluene under ambient conditions. The absorption of **1c** at 0 min is shown as an inset. Over the course of 41 h, with one spectrum taken every six hours, the NIR absorption decreases while a new vibronic absorption appears (onset at 550 nm).

and kept in a capped NMR tube, only minor decomposition was observed in the ^1H NMR spectrum after 24 h. Based on UV/Vis absorption, ^1H NMR spectroscopy, and FAB mass spectrometry results, we believe that **1c** undergoes photo-oxygenation to give a tetracene-containing structure **10** (Scheme 4). The growth of a new vibronic pattern with onset at 550 nm and the appearance of a signal with m/z 1075 $[M+H]$ in the FAB mass spectrum, corresponding to the dioxygen adduct of **1c**, suggested that a new oxidized species had formed (Figure 6). The formation of **10** was also shown by the change in solution color from brown to orange, which supports the presence of a tetracene moiety. Although the signal at m/z 1075 has the same m/z value as the starting material **8**, it arises from addition of an oxygen molecule to heptacene **1c** during analysis. The reason for this oxidation pattern can be deduced from analysis of the chemical structure of **1c**. Since the most reactive 7,16 positions are protected by the triisopropylsilyl ethynyl groups, the next reactive positions that are not functionalized can undergo



Scheme 4. Proposed structure of oxidation product.

oxidation, namely the 6,17 or 8,15 positions. By following the evolution of absorption patterns in the UV/Vis–NIR spectra, it is apparent that the reaction did not terminate with the addition of one molecule of oxygen. The absorptions at 535 nm decrease in intensity while the absorptions in the UV region intensify. It is very likely that both 6, 17 and 8, 15 positions underwent cycloaddition. The fact that no dimer was isolated, even after recrystallization for three weeks, indicates the effectiveness of phenyl groups in preventing self-reaction better of **1c**.

It appears that besides the steric hindrance imposed by the TIPS-acetylene groups (TIPS = triisopropylsilyl), it is also possible that electronic effects may have helped stabilize **1c**. This is a conclusion drawn from two observations. Firstly, according to the current proposed empirical model for engineering crystalline derivatives using an alkylsilylacetylene group, the solubilizing group needs to have a diameter of 35–50% of the length of the acene to have a significant stabilizing effect.^[12] However, the TIPS groups in **1c** are significantly smaller than the suggested range, yet the acene is the most stable in the group **1a–c**, as well as the reported bisTTMSS heptacene (TTMSS = tris(trimethylsilyl)silane).^[9] Secondly, the onset of the NIR absorption of **1c** is red-shifted by approximately 20 nm compared to compounds **1a** and **1b**, which indicates an electronic effect of the TIPS acetylene groups on the acene backbone (Figure 7).

The bandgap width was further confirmed by cyclic voltammetry (Figure 8). Heptacene **1c** has one reversible reduction at -1.13 eV and one reversible oxidation at 0.25 eV (vs. Ag/Ag^+ reference electrode). This results in a bandgap of 1.38 eV, which is in close agreement with the bandgap extrapolated from the Vis/NIR onset at 917 nm (1.35 eV). Although small molecules are expected to have a significant discrepancy between the electrochemical bandgap energies onset of electronic absorption, this heptacene derivative, with a molecular weight of 1042 Da, is large enough to be considered an equivalent of two oligoacetylenes, hence the general trend observed in small molecules is unlikely to be applicable, which explains the small discrepancy between the two methods for band gap determination. When the cyclic voltammetry (CV) experiment of **1c** was extended to 1 eV, a strong oxidation wave that was only partially reversible was observed. The HOMO and LUMO levels were calculated with ferrocene as internal standard to give a HOMO and LUMO levels of approximately -4.8 eV and -3.5 eV, respectively.

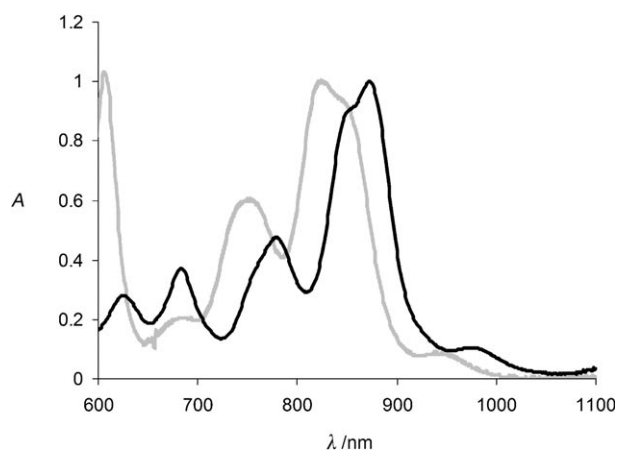


Figure 7. Bathochromic shift in the NIR absorption that results from the presence of TIPS groups in heptacene **1c** (solid line) compared to heptacene **1b** (dotted line).

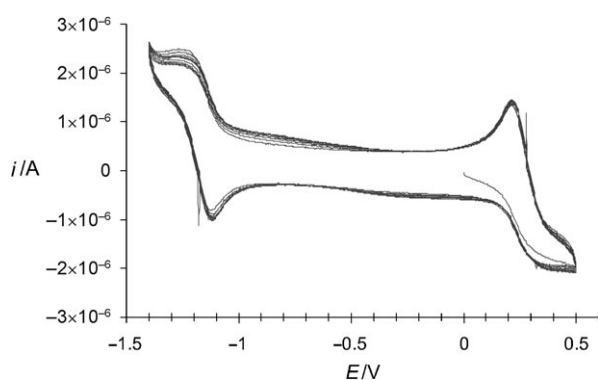


Figure 8. Cyclic voltammogram (vs. Ag/Ag^+) of **1c** with Bu_4NPF_6 in DCM solution (0.1 M), cycled 10 times.

Of the three heptacene derivatives synthesized, only the bis(alkylsilylethynyl)tetraphenyl derivative **1c** was sufficiently stable to allow characterization beyond UV/Vis–NIR spectroscopy. While phenyl groups are effective in preventing dimerization and polymerization of the longer acene, the central ring must be functionalized with alkylsilylethynyl groups in order to provide sufficient stability for isolation and characterization. Like pentacene, **1c** packs edge-to-face in single crystals. The band gap determined from CV and NIR onset supports the theoretical prediction of narrow but nonzero band gap;^[4,5] however, judging from the sharp NMR splittings and narrow line widths, if there is a singlet diradical character in the ground state,^[4,5] it is detectable only by the high reactivity of the molecules and not spectroscopically. As long as heptacene **1c** is protected from oxygen, it can be exposed to light, and will remain stable for extended periods. We are currently exploring the potential electronic applications of this exciting oligoacene.

Experimental Section

All general reagents were purchased from Aldrich and were used without further purification unless otherwise specified. Tetrahydrofuran was distilled from sodium and benzophenone and was used

immediately. $nBuLi$ was titrated with 2,2'-dipyridyl in anhydrous THF to determine the correct concentration prior to use. 1H and ^{13}C NMR spectra were recorded on a Bruker AVANCE500 spectrometer in $CDCl_3$ with tetramethylsilane as the internal standard, unless otherwise specified. Mass spectrometry data were obtained from a VG70 Magnetic Sector instrument in FAB mode. Electrochemical experiments were performed with a Princeton Applied Research Potentiostat/Gavanostat model 263A with Bu_4NPF_6 (0.1 M) in dichloromethane containing ferrocene as the internal standard. X-ray crystallographic analysis was carried out on a Bruker 3-axis platform diffractometer.

General procedure for the synthesis of **5a**, **5b**, and **8**: $nBuLi$ (1.30 mmol) was added dropwise to a separate solution of 2,2,6,6-tetramethylpiperidine (1.30 mmol) in dry THF (10 mL) at 0°C. The mixture was allowed to stir at 0°C for 20 min. The resulting lithium tetramethylpiperidide was slowly added by cannula (ca. 20 min) to a solution of 2,6-dibromoanthracene (0.216 mmol) and diphenylisobenzofuran (0.648 mmol) in dry THF (10 mL) at 0°C. This solution had been degassed by bubbling argon, which had been passed through activated oxygen-scavenger RIDOX and $CaSO_4$, for 30 min with protection from light. The reaction was allowed to proceed in the dark and to reach room temperature overnight, it was then quenched by pouring into 20 mL of saturated NH_4Cl , the aqueous layer was then extracted with ethyl acetate (3×10 mL). The combined organic layers were washed with water (2×15 mL), brine (1×15 mL) and then dried over $MgSO_4$. Upon evaporation of all solvents under reduced pressure on a rotary evaporator, the crude product was chromatographed on a SiO_2 column with an eluent gradient starting with hexanes, followed by 1–5% ethyl acetate in hexanes. Yield: 32–34%.

5a (syn and anti isomers): 1H NMR (500 MHz, $CDCl_3$): δ = 7.805–7.770 (m, 8H), 7.562–7.399 (m, 22H), 7.304–7.226 (m, 8H), 7.049 (dd, J_1 = 3 Hz, J_2 = 6 Hz, 2H), 7.018 ppm (dd, J_1 = 3 Hz, J_2 = 6 Hz, 2H) MS(FAB⁺): m/z 867.24 [$M+H$].

5b (syn and anti isomers): 1H NMR (500 MHz, $CDCl_3$): δ = 7.839–7.801 (m, 8H), 7.573, 7.537 ($2 \times$ s, 4H), 7.491–7.406 (m, 12H), 7.301 (dd, J_1 = 3 Hz, J_2 = 5.5 Hz, 3H), 7.179–7.125 (m, 4H), 7.087–7.010 (m, 7H), 6.957 (dd, J_1 = 2 Hz, J_2 = 8.5 Hz, 2H), 3.993 (dd, J_1 = 3 Hz, J_2 = 6 Hz, 4H), 1.576 (m, 2H), 1.445 (m, 16H), 1.056 (t, J = 7.5 Hz, 6H), 1.004 ppm (t, J = 7.5 Hz, 6H). MS(MALDI CH_2Cl_2/α -cyano-4-hydroxycinnamic acid) m/z 1123.7 [$M+H$].

8 (syn and anti isomers): 1H NMR (500 MHz, $CDCl_3$) δ = 8.399, 8.388 ($2 \times$ s, 4H), 8.030–8.006 (m, 8H), 7.603–7.565 (m, 8H), 7.515–7.493 (m, 4H), 7.456 (dd, J = 3 Hz, 2H), 7.432 (dd, J = 3 Hz, 2H), 7.085 (m, 4H), 1.162–1.118 ppm (m, 42H). ^{13}C NMR (500 MHz, $CDCl_3$): δ = 149.31, 149.28, 147.33, 135.09, 135.07, 131.93, 129.05, 128.45, 126.90, 126.73, 126.71, 120.87, 120.80, 119.63, 118.05, 104.52, 104.50, 103.51, 90.22, 19.09, 19.07, 11.61 ppm. MS (FAB⁺): m/z 1075 [$M+$] 1076 [$M+H$].

1c: Glacial acetic acid (0.5 mL) and zinc dust (<10 micron, ca. 50 mg, 0.76 mmol) was added to a suspension of bis-endo-oxide **8** (28 mg, 0.026 mmol) in toluene (10 mL) in a 25 mL Schlenk tube equipped with a stirrer bar. The mixture was degassed by three freeze-pump-thaw cycles and then heated to 100°C under argon for 4 days with protection from light. The reaction was monitored by the changes in the color of the solution over time; it was considered complete when the color was dark brown and exhibited no visible fluorescence. The hot reaction mixture was allowed to cool slowly in the oil bath in the dark. High quality opaque prismatic crystals (20 mg, 73% yield) were obtained after 3 weeks. 1H NMR (500 MHz, CD_2Cl_2): δ = 9.136 (s, 4H), 7.645 (t, J = 1.4 Hz, 8H), 7.575 (tt, J_1 = 1.3 Hz, J_2 = 7.4 Hz, 4H), 7.532 (dd, J_1 = 1.5 Hz, J_2 = 6.7 Hz, 8H), 7.3771 (dd, J_1 = 3.3 Hz, J_2 = 7 Hz, 4H), 7.107 (dd, J_1 = 3.3 Hz, J_2 = 7 Hz, 4H), 1.025 (d, J = 7.3 Hz, 36H), 0.874 ppm (m, 6H). ^{13}C -APT-NMR (500 MHz, $CDCl_3$): δ = 131.81, 129.24, 128.21, 127.63, 126.80, 125.68 (all aromatic CH), 19.14 (iPr CH_3), 12.12 ppm (iPr CH). MS (FAB): m/z 1042 [$M+$], 1043 [$M+H$], 1044 [$M+2H$]. UV/Vis/NIR (toluene): λ_{abs} = 355, 383, 437, 463, 696, 772, 863 nm.

1a and 1b: The procedure for the synthesis of **1a** and **1b** was the same as for **1c**. The only characterization data obtained for **1a** and **1b** are the UV/Vis absorption spectra described above.

X-ray single crystal structure analysis: The dark-brown heptacene crystal **1c** of approximate dimensions $0.25 \times 0.25 \times 0.2$ mm was mounted on a glass fiber and transferred to a Bruker CCD platform diffractometer. The SMART^[19] program was used to determine the unit cell parameters and data collection (15 sec/frame, 0.3 deg./frame for a sphere of diffraction data). The data were collected at 150 K using an Oxford nitrogen gas cryostream system. The raw frame data were processed using the SAINT^[20] program. Empirical absorption corrections were applied based on psi-scan. Subsequent calculations were carried out using SHELXTL^[21] program. The structure was solved by direct method and refined on F^2 by full-matrix least-squares techniques. Hydrogen atoms were located from the difference map. At convergence, $R_1 = 0.0641$ for 3207 reflections with $I > 2\sigma(I)$ and $GOF = 0.996$. $R_{int} = 0.0710$, $wR = 0.1267$. The orthorhombic crystals belong to space group *Pccn*, with $a = 28.481(8)$ Å, $\alpha = 90^\circ$, $b = 14.140(5)$ Å, $\beta = 90^\circ$, $c = 14.869(5)$ Å, $\gamma = 90^\circ$, $Z = 4$. CCDC 692899 contains the supplementary crystallographic data for this paper. These data can be obtained free of charge from The Cambridge Crystallographic Data Centre via www.ccdc.cam.ac.uk/data_request/cif

Received: July 10, 2008

Published online: September 29, 2008

Keywords: arynes · heptacenes · pericyclic reaction · polycycles · semiconductors

- [1] J. E. Anthony, *Angew. Chem.* **2008**, *120*, 460; *Angew. Chem. Int. Ed.* **2008**, *47*, 452.
- [2] M. Bendikov, F. Wudl, D. F. Perepichka, *Chem. Rev.* **2004**, *104*, 4891.
- [3] M. Faraday, *Philos. Trans. R. Soc. London* **1825**, 440.

- [4] M. Bendikov, H. M. Duong, K. Starkey, K. N. Houk, E. A. Carter, F. Wudl, *J. Am. Chem. Soc.* **2004**, *126*, 10493.
- [5] M. Bendikov, H. M. Duong, K. Starkey, K. N. Houk, E. A. Carter, F. Wudl, *J. Am. Chem. Soc.* **2004**, *126*, 7416.
- [6] D. E. Jiang, S. Dai, *J. Phys. Chem. A* **2008**, *112*, 332.
- [7] R. Mondal, R. M. Adhikari, B. K. Shah, D. C. Neckers, *Org. Lett.* **2007**, *9*, 2505.
- [8] R. Mondal, B. K. Shah, D. C. Neckers, *J. Am. Chem. Soc.* **2006**, *128*, 9612.
- [9] M. M. Payne, S. R. Parkin, J. E. Anthony, *J. Am. Chem. Soc.* **2005**, *127*, 8028.
- [10] M. S. Taylor, T. M. Swager, *Angew. Chem.* **2007**, *119*, 8632; *Angew. Chem. Int. Ed.* **2007**, *46*, 8480.
- [11] J. E. Anthony, J. S. Brooks, D. L. Eaton, S. R. Parkin, *J. Am. Chem. Soc.* **2001**, *123*, 9482.
- [12] J. E. Anthony, D. L. Eaton, S. R. Parkin, *Org. Lett.* **2002**, *4*, 15.
- [13] J. H. Chen, S. Subramanian, S. R. Parkin, M. Siegler, K. Gallup, C. Haughn, D. C. Martin, J. E. Anthony, *J. Mater. Chem.* **2008**, *18*, 1961.
- [14] S. K. Park, T. N. Jackson, J. E. Anthony, D. A. Mourey, *Appl. Phys. Lett.* **2007**, *91*, 063514.
- [15] C. D. Sheraw, T. N. Jackson, D. L. Eaton, J. E. Anthony, *Adv. Mater.* **2003**, *15*, 2009.
- [16] W. Steglich, E. Buschmann, G. Gansen, L. Wilschowitz, *Synthesis* **1977**, 252.
- [17] This dibromoanthracene derivative was synthesized under the same reaction condition as reported in Ref. [16], except instead of anthranilic acid, 5-bromoanthranilic acid was used.
- [18] J. H. Park, D. S. Chung, J. W. Park, T. Ahn, H. Kong, Y. K. Jung, J. Lee, M. H. Yi, C. E. Park, S. K. Kwon, H. K. Shim, *Org. Lett.* **2007**, *9*, 2573.
- [19] SMART Software Users Guide, Version 5.1, Bruker Analytical X-ray Systems, Inc., Madison, WI, **1999**.
- [20] SAINT Software Users Guide, Version 5.1, Bruker Analytical X-ray Systems, Inc., Madison, WI, **1999**.
- [21] Sheldrick, G. M. SHELXTL, Version 6.12, Bruker Analytical X-ray Systems, Inc., Madison, WI, **2001**.